Calculated effects of pressure-driven temperature oscillations on heat exchangers in thermoacoustic devices with and without a stack

Ray Scott Wakeland and Robert M. Keolian[a)]
The Pennsylvania State University, Graduate Program in Acoustics and Applied Research Laboratory, P.O. Box 30, State College, Pennsylvania 16804-0030

(Received 29 July 2003; accepted for publication 5 April 2004)

A Lagrangian computational method is used to explore the performance of heat exchangers in conditions of oscillating flow and oscillating pressure relevant to thermoacoustic devices. Pressure oscillations cause temperature oscillations within the working gas. Depending on phase, these ''pressure-driven temperature oscillations'' can enhance or degrade heat transfer within the exchangers of a thermoacoustic device. © *2004 Acoustical Society of America.*
[DOI: 10.1121/1.1755238]

PACS numbers: 43.35.Ud, 44.27.+g, 07.20.Pe [RR] Pages: 294–302

I. INTRODUCTION

This paper reports the results of a simple computational model for studying the combined effects of oscillating flow and oscillating pressure on the performance of heat exchangers in thermoacoustic devices. Originally motivated by our work on an unusual type of thermoacoustic device having neither stack nor regenerator, the model predicts effects that may be of considerable importance for heat exchangers in all types of thermoacoustic devices.

In a previous paper,[1] the authors developed a semianalytical model to examine the feasibility of ''no-stack'' thermoacoustic devices, consisting of two heat exchangers separated by a small gap and placed in a standing wave of high amplitude (>15% of mean pressure). The semianalytical model involves many assumptions, the most important being that the heat exchangers make perfect thermal contact with the oscillating gas, i.e., that the exchangers have an effectiveness of 100%. At the time that the model was developed, it was presumed that the imperfect performance of real heat exchangers would invariably degrade performance, but the magnitude of the effect was unknown. The present computational method was developed to explore the effects of imperfect heat exchangers on the efficiency of no-stack devices. The conclusions are somewhat startling: reducing heat exchanger effectiveness (from 100%) can actually *increase* the amount of heat pumped by a no-stack refrigerator. The effect comes about because of an interaction in the gas within an exchanger between temperature changes caused by thermal conduction and temperature changes caused by pressure oscillations. It is likely that this same mechanism has considerable influence on the performance of the heat exchangers in the more common sorts of thermoacoustic devices.

The computational model uses a time constant to characterize the degree of thermal contact between a Lagrangian parcel of gas and the exchanger. By removing pressure oscillations from the computation, it is possible to determine how effective each simulated exchanger would be in a simple oscillating flow, without externally imposed pressure oscillations. We have recently measured the effectiveness of parallel-plate heat exchangers in such oscillating flow,[2] so that it is now possible to match the relaxation parameter used in the model to the physical dimensions of real exchangers operating with laminar flows. The results support the validity of the one-dimensional model, and indicate that even heat exchangers that have very high effectiveness in pure oscillating flow are still subject to a large effect from pressure-driven temperature oscillations.

Because the oscillating-flow apparatus used for the measurements is incapable of imposing pressure oscillations, those measurements do not test experimentally the hypotheses of the present work. It is possible, however, to infer some experimental support for the idea from measurements on a working thermoacoustic refrigerator that have been described in a paper by Mozurkewich;[3] this evidence is presented in Sec. V.

Some potentially important physical phenomena are not included at all in the present model. Experiments carried out by Stephan Turneaure, a post-doctoral researcher working in this same laboratory, have already demonstrated one inadequacy in the method described in this paper. Turneaure's no-stack prime mover would reach onset and maintain oscillation at amplitudes such that no single parcel entered both exchangers. This outcome is not predicted by the model in this paper. The explanation of sustained, low-amplitude oscillations involves the thermal interactions *between* parcels, and this requires a calculation that tracks all of the parcels simultaneously as they oscillate. The computer programs used to generate the results of the present paper calculate the path of each parcel separately. This is a much simpler programming task, and we believe it is adequate to lend credence to the assertion that without inclusion of the contribution of pressure oscillations, any model of heat exchanger performance in thermoacoustic devices is incomplete.

II. THE COMPUTATIONAL MODEL

In a no-stack device, heat transfer and work consumption or production are carried out primarily by the volume of

a)Electronic mail: keolian@psu.edu

 0001-4966/2004/116(1)/294/9/$20.00

gas that enters both hot and cold heat exchangers. This volume of gas, the ''working gas,'' can be conceptually broken into thin transverse slices (''parcels''). If the heat exchangers are perfect, then all parcels perform equally, since all undergo identical, complete temperature changes upon entering either exchanger. To relax the assumption of heat-exchanger ideality, it is necessary to consider the parcels separately, since each spends a different amount of time in each of the two exchangers. Thus, an additional goal of the present calculation is to access the performance of parcels near the edges of the working gas, which spend a large fraction of the cycle in one exchanger but very little in the other.

The present model is as simple as possible. It is a one-dimensional model for parallel-plate heat exchangers. Individual parcels are taken to be lumped elements that undergo ordinary conductive thermal relaxation toward the exchanger temperature during periods when they are within an exchanger. The relaxation time is taken to be a constant, independent of velocity or position within the exchanger. Since the heat exchangers are imperfect, pressure oscillations cause temperature changes even in the gas that is within an exchanger. The oscillation period is partitioned into 1000 time steps. Within each small time step a thermal relaxation term is added to the temperature change that the gas *would have undergone* had it been adiabatic. Each parcel is treated independently. Thermal conduction between the parcels is neglected.

In a two-dimensional view, each parcel (slice) would be further divided along the transverse direction into many smaller units, called ''elements'' in the following discussion. The one-dimensional parcel approximation lumps the thermal decays of the various elements that make up a parcel into a single relaxation time, averaging over the faster decays of elements closer to a plate and the slower decays of those that are further away (viewing heat flow within the exchanger as the linear superposition of independent heat flows from each element). Effectively, we are using the average temperature of the elements of a parcel as the one-dimensional temperature of the model, assuming that the average over those elements is adequately described by a single exponential decay time.

Note that for laminar flow this averaging procedure is unaffected by the spatial distortion of the parcel into parabolic or other profiles because the distance from each element of the parcel to a plate remains the same. This holds as long as enough of the elements of the parcel are sufficiently far from the ends of the exchanger that end effects on the heat flow from an element to the exchanger can be neglected—a distance on the order of the gap between the plates, which is independent of velocity and should not be confused with the thermal or hydrodynamic entry lengths used in Eulerian heat exchange calculations. We therefore expect this one-dimensional approach to be an adequate approximation even when the flow is two-dimensional. The one-dimensional temperature T used in the model then becomes a label for the average of the temperatures of the fluid elements of a parcel of fluid that is a planar slice when it is between the exchangers and that distorts into another shape within the exchangers. The Lagrangian position of the parcel used in the model is the average position of its elements. The shape distortion may increase the thermal coupling between the parcels, which is neglected in the model, by bringing them into more intimate contact with each other. But since in the end we are interested in the total work and total heat transfer summed over all the parcels, this interparcel transfer of heat is assumed to be unimportant. Thus, we expect the model to be most reliable for parallel-plate heat exchangers that are long compared to the gap between the plates, and for parcel displacements into the exchangers that are larger than the gap but smaller than the plate length. Our use of a single relaxation time implicitly assumes that the thermal conductivity of the gas is constant.

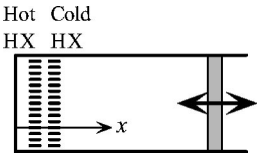

FIG. 1. Locations of the hot and cold heat exchangers.

With some care, it may be possible to adapt the results of the model to exchangers that have turbulent flow between the plates, shortening the average relaxation time because turbulent mixing brings elements into better overall thermal contact with the plates, but keeping in mind that our measurements were made using exchangers for which the flow was laminar (see Ref. 4, p. 150 for details).

In the FORTRAN program written to carry out the calculations, we use the following procedure: the extent of the working gas is determined; the working gas is divided into small parcels, each with its own displacement amplitude as well as its own mean position; the steady-state starting temperature for each parcel is determined by iterating until the cycle begins and ends at the same temperature; the heat and work are calculated for each individual parcel; and the total heat and work are calculated by adding up the contributions of all the working parcels. The equations are summarized in Sec. III. The complete FORTRAN code, along with detailed documentation, can be found in Ref. 4.

Other assumptions in the model are as follows.

(1) The model emulates the conditions in a cylinder of gas driven by a piston at a frequency that is well below the lowest acoustic resonance of the gas in the enclosure, so that, at each instant, the pressure is the same everywhere within the cylinder. This is the situation in a no-stack device [see Figs. 1, 2(a), and 7(a) of Ref. 1].

(2) The piston oscillates sinusoidally, and the gas acts as a gas spring undergoing uniform ''strain amplitude'' S, so that, for the gas parcel at mean position x_0 from the closed end of the cylinder,

$$x(x_0,t)=x_0+x_0 S \sin \omega t. \tag{1}$$

(3) The cylinder contains two heat exchangers, one hot and one cold, as shown in Fig. 1. As the gas is pushed back and forth, it contacts the two heat exchangers, which cause parcels of gas to change temperature, and therefore volume. A major assumption of the model used here is that the volume of the working gas is such a small fraction of the total

volume of the cylinder that these temperature-induced volume fluctuations have negligible effect on the pressure in the cylinder. As the pressure in the cylinder varies in time, the location $x(t)$ of the parcel that has equilibrium position x_0 varies, so that the instantaneous pressure and position of the parcel are related by the adiabatic gas law according to

$$p(t)=p_0\left(\frac{x}{x_0}\right)^{-\gamma}=p_0(1+S\sin\omega t)^{-\gamma}, \tag{2}$$

where p_0 is the quiescent pressure and γ is the ratio of specific heats, c_p/c_v. This assumption is equivalent to a common thermoacoustics approximation that the heat exchangers operate in a pure standing wave, with negligible traveling-wave component. This approximation is used in Ref. 1 as well. The main consequence for the computation is that it is not possible to calculate work input or output at the piston. Instead, work must be calculated from the difference in the magnitudes of the input and output heats.

III. METHOD OF CALCULATION

There are three types of regions: between the heat exchangers, within the exchangers, and beyond the exchangers. Regions between and beyond the exchangers are adiabatic. The regions where the gas is within the exchangers are the ones that require numerical time stepping. The rate of thermal relaxation is given by a time constant τ, such that

$$\Delta T_{\text{relaxation}}=-(T-T_{\text{hx}})\frac{\Delta t}{\tau}, \tag{3}$$

where Δt is the time step and T_{hx} is the heat exchanger temperature. For an adiabatic, ideal gas,[5] $pV=mRT$ and $pV^{\gamma}=p_0V_0^{\gamma}$, so that

$$\frac{\Delta T_{\text{adiabat}}}{T}=\frac{\gamma-1}{\gamma}\frac{\Delta p}{p}. \tag{4}$$

Thus, the model of heat exchange propounded here is summarized by

$$\Delta T=\Delta T_{\text{adiabat}}+\Delta T_{\text{relaxation}} \tag{5}$$

$$=\left[\frac{\gamma-1}{\gamma}\frac{T\tau}{p}\frac{dp}{dt}-(T-T_{\text{hx}})\right]\frac{\Delta t}{\tau}. \tag{6}$$

Volume changes are calculated from the ideal gas law,

$$\frac{dV}{V}=\frac{dT}{T}-\frac{dp}{p}. \tag{7}$$

Separate heats from the cold exchanger and the hot exchanger (Q_{cold} and Q_{hot}) are calculated using

$$dQ=-C_p(T-T_{\text{hx}})\frac{dt}{\tau}, \tag{8}$$

where $C_p=mR\gamma/(\gamma-1)$, with m being the mass of the gas in the parcel. The net work produced by the cycle is $W_{\text{net}}=Q_{\text{hot}}+Q_{\text{cold}}$.

We can estimate the relation between τ and the parameters of a parallel-plate heat exchanger with a simple "RC" thermal model. The gas filled gap between the plates is $2y_0$. The characteristic distance that heat can diffuse in $1/\pi$ of an acoustic period is called the thermal penetration depth $\delta_\kappa=\sqrt{k_0/\rho_m c_p \pi f}$, where f is frequency, k_0 is the thermal conductivity, ρ_m is the mean density, and c_p is the isobaric specific heat of the gas. If the wetted area of a parallel-plate exchanger is A and the film thickness is δ_κ for $\delta_\kappa<y_0$, then the thermal "capacitance" of the gas in the exchanger is $\rho_m c_p y_0 A$ and the "resistance" is $\delta_\kappa/k_0 A$, their product giving a time constant τ such that

$$\tau f\simeq\frac{1}{\pi}\frac{y_0}{\delta_\kappa} \tag{9}$$

for large values of τf or y_0/δ_κ. For small values of y_0/δ_κ we may expect that the thermal capacitance is given by the same expression, but that the length in the resistance might have an upper limit of approximately $y_0/2$, so that the resistance becomes $y_0/2k_0A$, resulting in

$$\tau f\simeq\frac{1}{2\pi}\frac{y_0^2}{\delta_\kappa^2} \tag{10}$$

for small values of τf or y_0/δ_κ.

IV. RESULTS

A. No-stack refrigerator

In the following, we use the parameters from our previous semianalytical model of an optimized no-stack refrigerator as inputs to the present time-stepping model. In that semianalytical model, these parameters resulted in model performance of $\dot{Q}_{\text{inviscid}}=1190\,\text{W}$, $\eta_{\text{II}_{\text{inviscid}}}=60.6\%$, and $\eta_{\text{II}_{\text{net}}}=38.0\%$ at $P_A/p_m=26.0\%$, where η_{II} is the second-law efficiency, which compares the coefficient of performance of the refrigerator to that of a Carnot refrigerator, and the subscripts "net" and "inviscid" indicate whether or not viscous losses are included in the calculation. As applied to the present time-stepping model, the relevant values, adapted from Tables I and III of Ref. 1, are: $p_0=2.07\,\text{MPa}$, $\gamma=1.667$, $f=320\,\text{Hz}$, $T_{\text{hot}}=303.1\,\text{K}$, $T_{\text{cold}}=276.9\,\text{K}$, $x_{\text{hot}}=0.012\,97\,\text{m}$, $x_{\text{cold}}=0.016\,12\,\text{m}$, $x_0=0.014\,55\,\text{m}$, $A_{\text{fr}}=0.0095\,\text{m}^2$, and $S=0.1487$, where x_{hot} and x_{cold} are the locations of the inside edges of the heat exchangers, T_{hot} and T_{cold} are the exchanger temperatures, A_{fr} is the cross-sectional area of the device, and S is the strain amplitude of Eq. (1). For these parameters,[6] the present time-stepping model produces the results in Fig. 2.

Figures 2(a) and (b) are the temperature-versus-position plot (Tx diagram) and the pV diagram for the centered parcel, the parcel that has an equilibrium position halfway between the inner edges of the exchangers. The heavy gray lines in the Tx diagram represent the temperatures and locations of the heat exchangers. Markers highlight the places where the parcel enters and exits the exchangers, and the points of maximum and minimum excursion. The asterisk marker shows the equilibrium position of the parcel in the x direction, while in the T direction it shows the start and end of the iterated cycle, where the matching condition on temperature must be met. For refrigerators, the parcel goes around these closed paths in a counterclockwise direction.

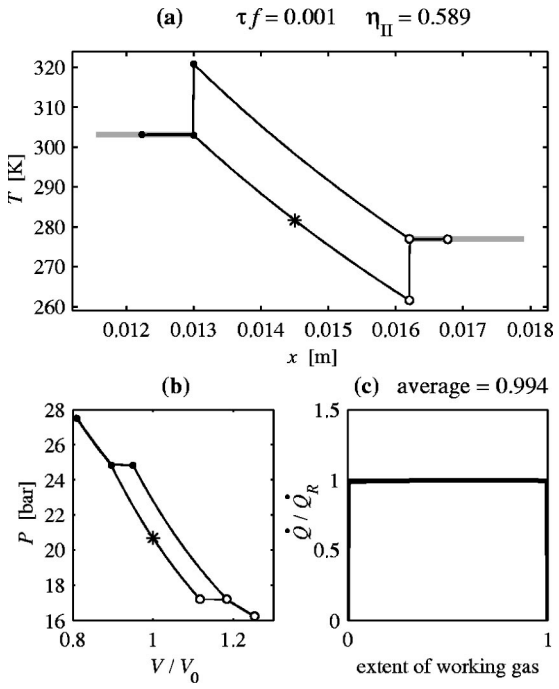

FIG. 2. Center-parcel results for the no-stack refrigerator with $\tau f = 0.001$. This is the smallest possible value of τf for the number of time steps used, so effectively $\tau f \simeq 0$.

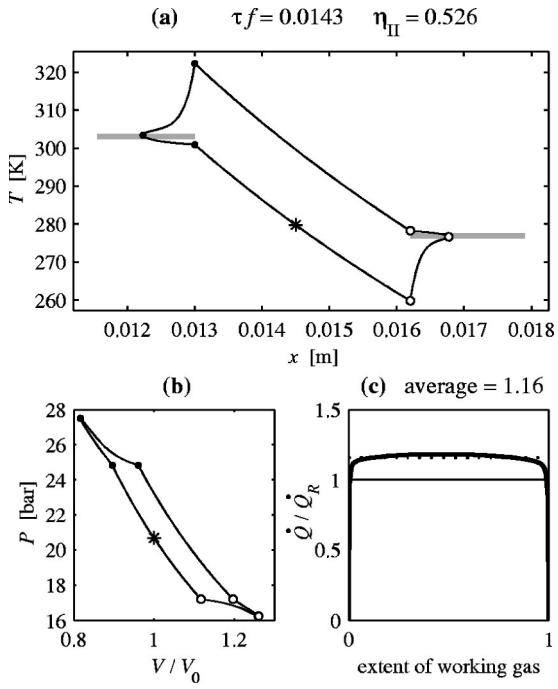

FIG. 3. Center-parcel results for the no-stack refrigerator with $\tau f = 0.0143$.

Figure 2(c) summarizes the results for the entire extent of the working fluid. The time-averaged rate of heat removal from the cold exchanger $\dot{Q}$ calculated by the time-stepping model is divided by the reference value $\dot{Q}_R = 1190\,\mathrm{W}$, the inviscid performance of the idealized refrigerator from the semianalytical model at this amplitude. In this simulation, the working gas is partitioned into 100 parcels. The results for each of the 100 parcels are plotted from left to right along the abscissa, with the left-most parcel of the working gas at 0 and the right-most parcel at 1. For each parcel, the heavy curve shows the magnitude of the rate at which heat would have been removed from the cold exchanger had every parcel performed equally with this parcel. This normalization makes it easy to compare the performance of each parcel to the *average* performance of the entire working volume, which is shown by a dotted horizontal line. [This line is obscured in plots with $\tau f \simeq 0$, since each parcel performs nearly identically, but is visible in part (c) of the other figures.] There is also a light-weight line at $\dot{Q}/\dot{Q}_R = 1$. The result for the time-stepped computation is not identical to that from the semianalytical model because the models are not identical—there is no linearization of the oscillating pressure in the time-stepped model, and there are small numerical errors. However, the average heat transfer result [printed above part (c)] agrees with the semianalytical model to 0.6%, and the inviscid second-law efficiency $\eta_{\mathrm{II}_{\mathrm{inviscid}}}$ [printed above part (a) simply as η_{II}, since this is an inviscid computation] agrees to 3%.

Figure 3 shows the result of slightly reducing the degree of thermal contact of the exchangers by increasing the normalized time constant to $\tau f = 0.0143$. In the Tx diagram of Fig. 3(a), we can follow the temperature of the gas as it decays toward the exchanger temperatures. Because the thermal contact is still excellent, near the extremes of displacement the temperature comes to the temperature of the exchanger. Then, as the gas moves back out of, say, the hotter exchanger, the declining pressure reduces the temperature of the gas, and the imperfect exchanger cannot hold the gas to its temperature. The gas exits this exchanger *colder* than it left the ideal exchanger; the rate of heat transport has been increased.

It is not so for all parcels. For any but perfect exchangers, the parcels at the edge of the working gas must transport zero heat, since they spend zero time in one exchanger or the other. Figure 3(c) shows the performance of the parcels near the edges falling off toward zero. For this excellent thermal contact, however, the great majority of parcels perform better than they did with ideal exchangers, with the net result that 16% more heat is removed from the cold exchanger. This is one of the primary results of this paper.

There is a cost to the enhancement. The second-law inviscid efficiency $\eta_{\mathrm{II}_{\mathrm{inviscid}}}$ has dropped 11%. This is also seen in the ''opening up'' of the pV diagram in Fig. 3(b). The enclosed area represents the amount of work done per cycle. In contrast to the corresponding diagram in Fig. 2(b), net work is being done even while the parcel is within the exchangers.

Similar results are shown for increasing τf in Figs. 4–6. Figure 4 shows the results for $\tau f = 0.0455$, the value at which $\dot{Q}$ reaches its maximum value, 33% higher than the value obtained for ideal exchangers, with an inviscid efficiency that is 77% of that for the ideal exchangers.

The value $\tau f = 0.136$ in Fig. 5 is interesting because the average heat pumping is the same as for ideal exchangers. The inviscid efficiency is down by almost 28% from its peak value. These are *inviscid* efficiencies, however. Presumably there is some cost in exchanger viscous loss and minor loss

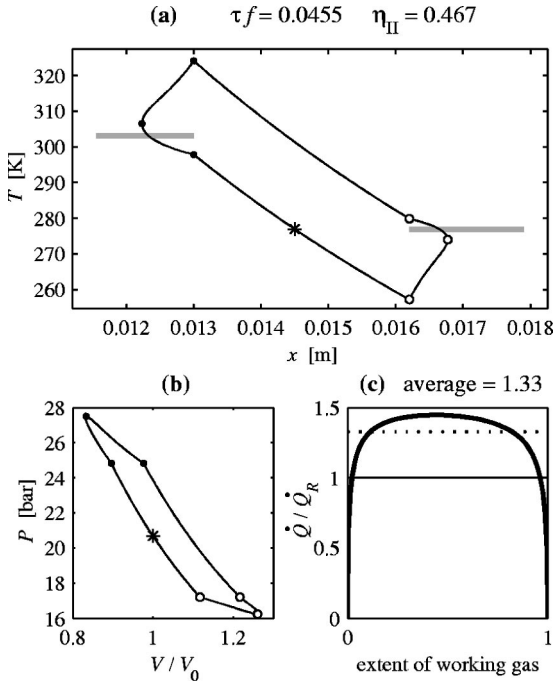

FIG. 4. Center-parcel results for the no-stack refrigerator with $\tau f = 0.0455$, which maximizes the average value of $\dot{Q}$.

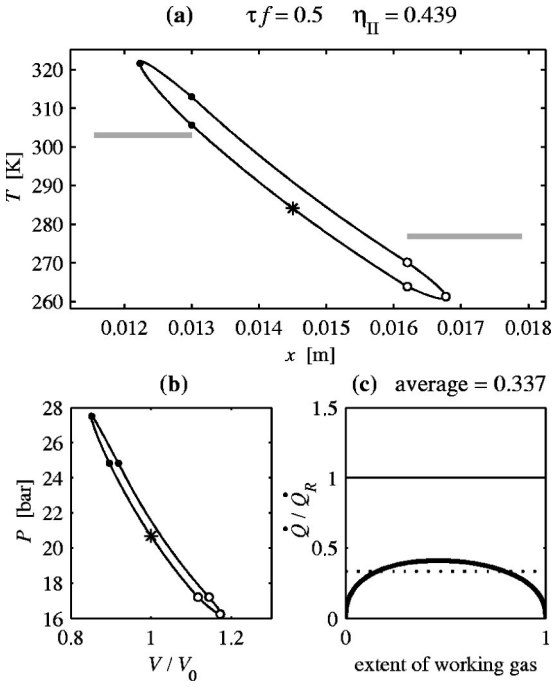

FIG. 6. Center-parcel results for the no-stack refrigerator with $\tau f = 0.5$.

to an exchanger that has nearly perfect thermal contact, so it is not immediately apparent which configuration would have the best *net* efficiency.

Comparing Fig. 4(c) to Fig. 5(c), the performance of off-center parcels has fallen faster than that of the centered parcel as τf has increased from 0.0455 to 0.136.

Finally, Fig. 6 shows the results for poor thermal contact, with $\tau f = 0.5$. The parcel path in xT space has begun to collapse toward the curve that results from adiabatic compression and expansion.

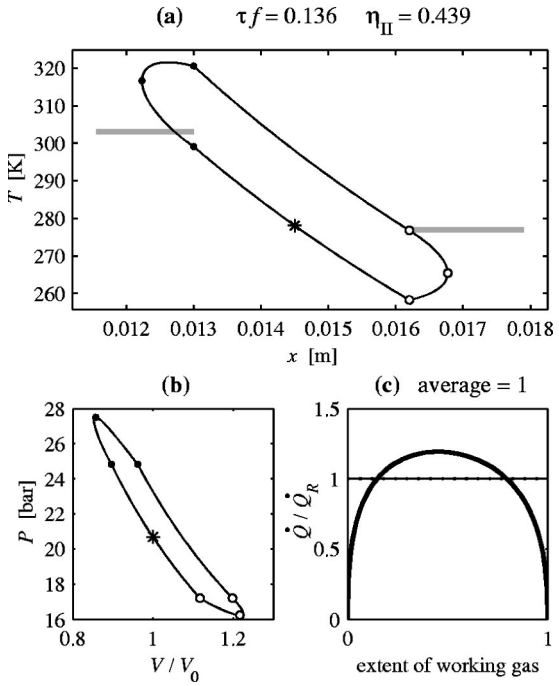

FIG. 5. Center-parcel results for the no-stack refrigerator with $\tau f = 0.136$.

B. Adjacent exchangers with no pressure oscillations: Correlation of τf with y_0/δ_κ

In our FORTRAN code, we provide for the possibility "turning off" the pressure oscillations (and the associated temperature oscillations) while leaving the displacement oscillations the same. This produces a simulation similar to the situation used to make the heat exchanger measurements in Ref. 2. Essentially, that experiment consisted of placing two parallel-plate heat exchangers, at different temperatures, close together, forcing air back and forth between them, and measuring the rate of heat transfer from the hot to the cold heat exchanger. By matching the measured effectiveness of the real heat exchangers to the effectiveness that is calculated using the present method, we can match values of τf from the model to values of the physical parameter y_0/δ_κ. "Effectiveness" is the ratio of the actual rate of heat transfer to the maximum possible heat transfer for a given temperature difference and heat capacity flow rate, and it is quite useful for analyzing heat exchangers in oscillating flow, as shown in Ref. 2.

For this comparison, we may set the parameters to any convenient values, provided that the exchangers are long enough. We then calculate $\dot{Q}$ divided by the value of $\dot{Q}$ obtained for $\tau f \simeq 0$, giving the combined effectiveness of the two-exchanger system. Figure 7 shows zero-pressure-amplitude results for $\tau f = 0.216$, which produces a combined, total effectiveness for the two-exchanger system of $[\epsilon_T]_{hx} = 70\%$. In the measurements,[2] this same effectiveness was observed for heat transfer between two adjacent parallel-plate heat exchangers for $y_0/\delta_\kappa = 1.0$. By running this heat-exchanger-measurement simulation at many different values of τf, the correspondence between τf and y_0/δ_κ can be mapped, as shown in Fig. 8. The values denoted by the + signs are based measurements of effectiveness which we

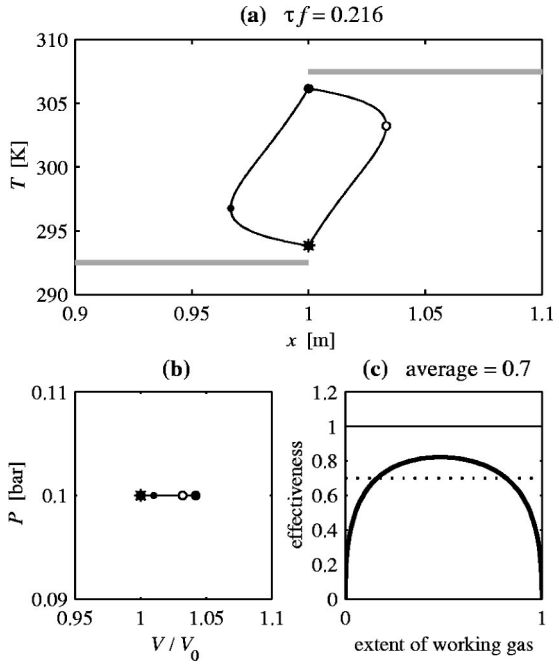

FIG. 7. Computational model of adjacent exchangers with no pressure oscillations for $\tau f = 0.216$. For this case, with no gap between the exchangers and no pressure oscillations, the average value $\dot{Q}/\dot{Q}_R$ corresponds to the total *effectiveness* $[\epsilon_T]_{\mathrm{hx}}$ measured in Ref. 2. The parcel follows a counterclockwise path in the *Tx* diagram.

judge to be somewhat less reliable than the others.[4] For large y_0/δ_κ, the correspondence is $\tau f = (1/3.487) y_0/\delta_\kappa$, indicated by the diagonal line. The constant 1/3.487 is smaller by 10% than the value $1/\pi$ that was predicted by the simple relaxation model, Eq. (9). At small τf there is a suggestion of a transition to the behavior described by Eq. (10), which is shown by the dashed curve. We see then that the one-dimensional model, together with rather crude estimates of the time constants, does a good job of reproducing the effectiveness results of the experiment performed without pressure oscillations. This bolsters our confidence that we can draw reasonable conclusions from the model predictions of situations that include pressure oscillations, particularly if we use the measurements to correct the correspondence between the plate spacings and the time constants.

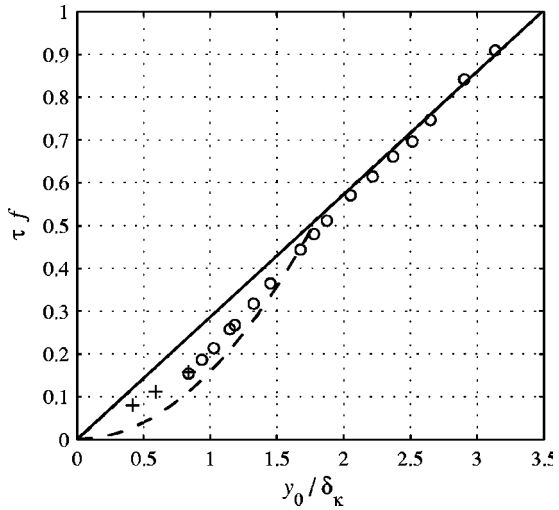

FIG. 8. Correspondence between y_0/δ_κ and τf, determined by matching the overall effectiveness $[\epsilon_T]_{\mathrm{hx}}$ measured for y_0/δ_κ and computed for τf. The values denoted by the + signs are based on less reliable measurements of effectiveness. The straight diagonal fit line is $\tau f = 0.90(y_0/\pi\delta_\kappa)$, a 10% correction on Eq. (9), which was used to estimate τf for large y_0/δ_κ. The dashed curve is Eq. (10), $\tau f = y_0^2/2\pi\delta_\kappa^2$, which was expected to approximate τf for small y_0/δ_κ.

For the values of τf shown in the figures, $\tau f = 0.0143$, 0.0455, 0.136, 0.216, and 0.500, the effectivenesses are $[\epsilon_T]_{\mathrm{hx}} = 0.999$, 0.981, 0.848, 0.700, and 0.379, respectively, with values of plate spacing $y_0/\delta_\kappa = 0.07$, 0.25, 0.76, 1.0, and 1.85 obtained by interpolating the data of Fig. 8. The correspondences for the smallest of these, $y_0/\delta_\kappa = 0.07$ and 0.25, are relatively uncertain.

What is striking about the results is just how sensitive the no-stack device is to small changes in effectiveness. For $\tau f = 0.0143$, the effectiveness *without* pressure oscillations is 99.9%, with a regenerator-like $y_0/\delta_\kappa \simeq 0.07$, yet this level of τf produces effects that are clearly visible in Fig. 3, and causes a 16% increase in total heat transport. The value $\tau f = 0.0455$, which maximizes heat transport in the no-stack refrigerator, has an effectiveness of 98.1% without pressure oscillations, corresponding to $y_0/\delta_\kappa \simeq 0.25$. The value $\tau f = 0.136$, which gives $\dot{Q}/\dot{Q}_R = 1$ in the no-stack refrigerator in Fig. 5(c), corresponds to $y_0/\delta_\kappa = 0.76$. This is not much greater than the value $y_0/\delta_\kappa = 0.63$ used in the calculation of overall efficiency in the semianalytical model of Ref. 1. In that paper, we assumed that $y_0/\delta_\kappa = 0.63$ would give "excellent thermal contact" in the heat exchangers, and it *does* in the absence of pressure oscillations, with $[\epsilon_T]_{\mathrm{hx}} = 90.4\%$, but the influence of the large pressure oscillations required in the no-stack refrigerator makes this a *minimum* value of effectiveness for high efficiency in that type of device.

When we first saw the result that decreasing the effectiveness of the exchangers in a no-stack refrigerator could increase heat pumping, we imagined that this might provide an opportunity to increase *net efficiency*, since looser exchangers would have lower viscous and minor losses. With the abstract quantity τf now connected to physical dimensions, though, it becomes apparent that the loosest of these "looser" exchangers is about what was already used in our previous modeling, so the hoped-for improvement is unrealizable. The value $y_0/\delta_\kappa = 0.63$ used in Ref. 1 corresponds to $\tau f = 0.104$. In the time-stepping model, this produces a heat-pumping enhancement of 15% but drops the inviscid efficiency by 27%. Substituting the time-stepping results into the semianalytical model of Ref. 1 drops the overall coefficient of performance relative to Carnot from $\eta_{\mathrm{II}_{\mathrm{net}}} = 38\%$ to 32%. In other words, the previous model was overly optimistic, assuming nearly perfect heat transfer with a spacing of $y_0/\delta_\kappa = 0.63$, which turns out actually to be fairly "loose" in the context of such a large pressure amplitude.

C. No-stack engines

The results for no-stack engines are equally interesting, but also somewhat disheartening. The no-stack refrigerator of the previous section can be converted into an engine by increasing the temperature difference between the exchangers. For this example, the temperature difference is increased

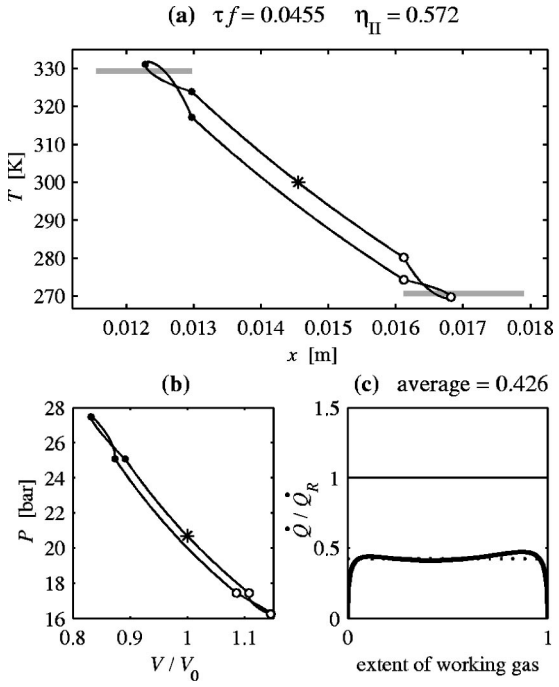

FIG. 9. Center-parcel results for no-stack engine with $\tau f = 0.0455$. Note that, in contrast to similar diagrams for refrigerators, the paths in Figs. 9(a) and (b) go clockwise, and $\dot{Q}$ and $\dot{Q}_R$ are taken at the hot heat exchanger.

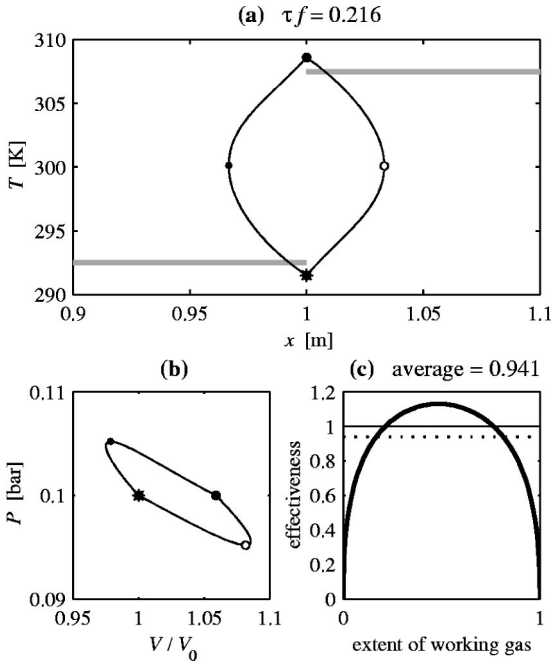

FIG. 10. The heat exchanger on the left corresponds to the hot heat exchanger in a stack-based refrigerator, here operated at an amplitude of 5% of mean pressure. The heat exchanger on the right corresponds to the hot end of the stack. The parcel follows a counterclockwise path in the Tx and pV diagrams.

until the heat input is $\dot{Q}_R = 1.18\,\mathrm{kW}$ for $\tau f = 0.001$. The value of τf is then increased to 0.0455, producing Fig. 9. This is the same value of τf as for the refrigerator in Fig. 4, but the effect is even more dramatic on the engine than on the refrigerator—the heat input, and the corresponding work output, are cut by more than half. Interestingly, $\eta_{\mathrm{II}_{\mathrm{inviscid}}}$ drops only 8%. When τf is reduced to 0.136 (not shown), the heat input is reduced to 13% of the original.

D. Heat exchangers in stack-based devices

With the FORTRAN program we can also illuminate the possible influence of pressure-driven temperature oscillations on the performance of heat exchangers in ordinary thermoacoustic devices. In Figs. 10 and 11, conditions have been selected so that when the pressure oscillations are "turned on," this same gas stroke generates a pressure amplitude that is 5% of the mean pressure, typical of stack-based devices.

Recall that Fig. 7 shows the selection of $\tau f = 0.216$, with $[\epsilon_T]_{\mathrm{hx}} = 70\%$, and corresponding to $y_0/\delta_\kappa = 1.0$, without pressure oscillations. Figure 10 shows the same gas motion, but with 5% pressure oscillations. The pressure increases as the gas moves *to the left*. Thus, the heat exchanger on the left, at 292.5 K, represents the ambient (exhaust) exchanger in a stack-based refrigerator, and the hotter exchanger on the right represents the hot end of the stack. The pressure oscillations cause fluctuations in temperature that raise the rate of heat removal from the stack to $0.941\,\dot{Q}_R$, an increase of 35%. Values of τf greater than 0.188 (corresponding to $y_0/\delta_\kappa = 0.95$) result in heat transfer exceeding what would be achieved with an ideal exchanger, peaking at an effectiveness value of 1.15 for $\tau f = 0.077$ (or $y_0/\delta_\kappa = 0.5$). We see from the pV diagram that work is required to achieve this enhancement.

In Fig. 11, the temperatures are reversed, but the pressure still increases as the gas moves to the left. This situation is similar to that of a hot (input) exchanger in a stack-based *engine*, with the colder exchanger on the right now repre-

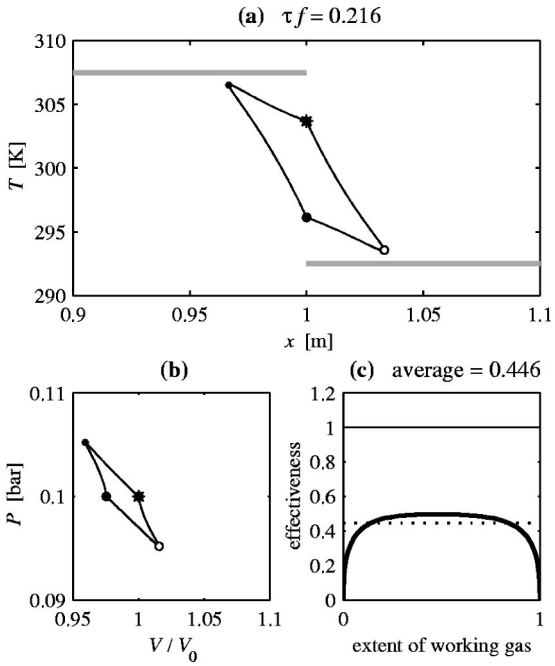

FIG. 11. The heat exchanger on the left corresponds to the hot heat exchanger in a stack-based engine, here operated at an amplitude of 5% of mean pressure. The heat exchanger on the right corresponds to the hot end of the stack. The parcel follows a clockwise path in the Tx and pV diagrams.

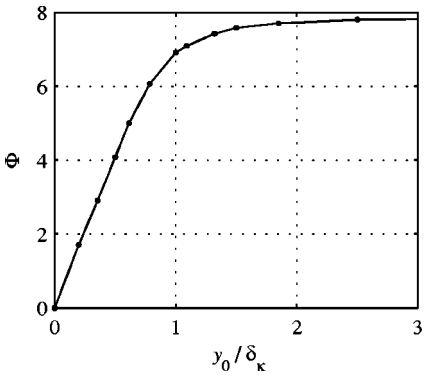

FIG. 12. Function Φ used in Eq. (11) to describe the amount of enhancement (or degradation) expected in a standing-wave thermoacoustic refrigerator (or engine).

senting the hot end of the stack. The gas now enters the hotter region while the pressure increases, and in this case the rate of heat transport *drops* by 35% compared with the same situation in the absence of the 5% pressure oscillation.

In the refrigerator-like situation, as the gas enters the left exchanger (which represents the ambient exchanger of the refrigerator), the increasing pressure tends to keep the gas temperature farther above the exchanger temperature in the period of time just after the gas enters the exchanger, thus increasing the average gas-to-exchanger temperature difference during this crucial part of the cycle. In the engine-like situation, increasing pressure tends to drive the temperature of the gas quickly toward the (left) exchanger temperature, decreasing the average temperature difference.

The amount of heat-transfer enhancement for stack-based refrigerators is about the same magnitude as the degradation for stack-based engines. The enhancement of heat transfer (either plus or minus) caused by pressure oscillations depends on both oscillation amplitude and τf. For a given value of τf, the amount of enhancement grows linearly with amplitude. That is, if $[\epsilon_T]_{\mathrm{hx}}$ is the effectiveness in the absence of pressure oscillations, then apparent effectiveness $[\epsilon_T]_{\mathrm{apparent}}$ in the presence of pressure oscillations is

$$[\epsilon_T]_{\mathrm{apparent}} = [\epsilon_T]_{\mathrm{hx}} \left(1 \pm \Phi \frac{p_A}{p_0} \right), \tag{11}$$

where p_A is the pressure amplitude and Φ is a function that depends on y_0/δ_κ, plotted in Fig. 12. The function Φ grows linearly for small y_0/δ_κ, eventually approaching a constant value of about 8. The values of y_0/δ_κ plotted in Fig. 12 are determined from τf using the correspondence plotted in Fig. 8. Note that Eq. (11) assumes that the stack and heat exchanger have the same value of y_0/δ_κ, which will often not be the case in an actual device.

In all of the above-mentioned examples, the exchangers are long enough that none of the working gas ever goes *beyond* either exchanger. The degree of influence of the pressure oscillations is smaller for exchangers shorter than the peak-to-peak gas displacement, since the gas spends less time interacting with the exchangers.

V. EVIDENCE IN SUPPORT OF THE MODEL

Mozurkewich has recently carried out measurements of heat transfer between a thermoacoustic stack and a tube heat exchanger within a thermoacoustic refrigerator.[3] The test heat exchanger was the one nearer the velocity node, the ''hot heat exchanger'' in a standing-wave refrigerator, which exhausts heat from the stack. Mozurkewich measured the amount of exhaust heat, the temperature T_{hhx} of the heat exchanger, and the temperature T_H of the stack material at the end of the stack adjacent to the exchangers. One of his interesting observations was of significant heat transfer when $T_H - T_{hhx}$ was *zero*. In Mozurkewich's experiments, this ''heat flow at zero temperature difference'' grew linearly with amplitude, as in his Fig. 2. (In this standing-wave type of device, displacement amplitude and pressure amplitude increase together.) By adjusting the temperature of the heat exchanger at the opposite end of the stack, he could bring the heat transfer to zero by forcing the temperature of the stack to be many degrees *below* that of the exchanger to which it was exhausting heat.

Clearly, a heat transfer model where $\dot{Q}$ is proportional to the temperature difference between the exchanger and the end of a stack or regenerator cannot account for this type of phenomenon, even when calibrated against oscillating-flow heat transfer experiments like the ones in Ref. 2, that do not include pressure oscillations. Further study may reveal some simple way to add pressure-amplitude-dependent terms to this type of model, along the lines of Eq. (11), but it may be necessary to incorporate a calculational model such as the one used here into the design software. David Gedeon's Sage software[7] uses a method that accounts for time-dependent temperature differences between gas and heat exchanger. It is not a time-stepping method, however, but rather a ''globally implicit'' method.[8] It would be quite instructive to compare the results of Sage modeling to those of the simple model presented here.

Of course, measurements are necessary to validate the ideas put forward in this paper. Such experiments would require a device similar to an alpha Stirling engine. For purposes of unambiguous analysis and interpretation, however, it would be better if this apparatus did not have a regenerator, but simply two heat exchangers, as in a no-stack refrigerator.

VI. CONCLUSIONS

The main purpose of this paper is to convey our conviction that pressure-driven temperature oscillations play an important role in the performance of heat exchangers in thermoacoustic devices. This means that the heat exchanger measurements and analysis of Ref. 2 are less definitive than they might appear.

The original motivation for this study was to examine the consequences for the no-stack model. The full implications were not exposed until the recent analysis of the heat exchanger measurements. The conclusions are rather negative for no-stack devices, suggesting that *extremely* effective heat exchangers would be required for efficient operation of

a no-stack refrigerator, and that the idea of a high-power no-stack engine may be unrealistic.

Regardless of the future of no-stack devices, the undertaking has been valuable because of the important implications for conventional thermoacoustic devices. It appears that the exchangers in standing-wave refrigerators probably receive a substantial boost in performance from the effects of pressure-driven temperature oscillations, and vice versa for standing-wave engines. The implications for regenerator-based devices have yet to be worked out.

The simple one-dimensional thermal relaxation model used here seems to work well even though this is a two-dimensional laminar flow. With further refinement of the time history of heat transfer from a parcel to the exchanger plates, the calculation should become nearly exact. We find that it is sometimes clearer to take a Lagrangian point of view in the time domain rather than to take the traditional Eulerian point of view in the spatial domain with its focus on hydrodynamic and thermal entry lengths.

ACKNOWLEDGMENTS

This work was supported by the Office of Naval Research, the Penn State Applied Research Laboratory, and the Pennsylvania Space Grant Consortium.

[1] R. S. Wakeland and R. M. Keolian, "Thermoacoustics with idealized heat exchangers and no stack," J. Acoust. Soc. Am. **111**, 2654–2664 (2002).

[2] R. S. Wakeland and R. M. Keolian, "Effectiveness of parallel-plate heat exchangers in thermoacoustic devices," J. Acoust. Soc. Am. (to be published).

[3] G. Mozurkewich, "Heat transfer from transverse tubes adjacent to a thermoacoustic stack," J. Acoust. Soc. Am. **110**, 841–847 (2001).

[4] R. S. Wakeland, "Heat exchangers in oscillating flow, with application to thermoacoustic devices that have neither stack nor regenerator," Ph.D. thesis, The Pennsylvania State University, 2003.

[5] In the version of the ideal gas law used here, m is the mass of the gas and R is the gas constant. The gas constant is defined such that $mR=nR$, where n is the number of moles in the parcel and R is the universal gas constant.

[6] Because p varies nonlinearly with x in the present model, we have used the displacement amplitude to match the two models.

[7] D. Gedeon, "Sage: Stirling-cycle model class reference guide," Gedeon Associates, 16922 South Canaan Rd., Athens, OH 45701 (1999).

[8] D. Gedeon, "A globally-implicit Stirling cycle simulation," in *Proceedings of the 21st IECEC* (American Chemical Society, Washington, DC, 1986), pp. 550–554.